THE JOURNAL OF BIOLOGICAL CHEMISTRY VOL. 285, NO. 43, pp. 33463–33474, October 22, 2010

Elucidation of a Novel Extracellular Calcium-binding Site on Metabotropic Glutamate Receptor 1α (mGluR1α) That Controls Receptor Activation*[S]

Received for publication, May 20, 2010, and in revised form, July 29, 2010 Published, JBC Papers in Press, August 12, 2010, DOI 10.1074/jbc.M110.147033

Yusheng Jiang[‡], Yun Huang[‡], Hing-Cheung Wong[‡], Yubin Zhou[‡], Xue Wang[§], Jun Yang[¶], Randy A. Hall[‖], Edward M. Brown[**], and Jenny J. Yang[‡1]

From the [‡]Department of Chemistry and the [§]Department of Computer Science, Center for Drug Design and Advanced Biotechnology, Georgia State University, Atlanta, Georgia 30303, the [¶]Department of Toxicology, Hangzhou Normal University School of Public Health, Hangzhou, Zhejiang 310036, China, the [‖]Department of Pharmacology, Emory University School of Medicine, Atlanta, Georgia 30322, and the [**]Division of Endocrinology, Diabetes, and Hypertension, Department of Medicine, Brigham and Women's Hospital, Boston, Massachusetts 02115

Metabotropic glutamate receptor 1α (mGluR1α) exerts important effects on numerous neurological processes. Although mGluR1α is known to respond to extracellular Ca^{2+} ($[Ca^{2+}]_o$) and the crystal structures of the extracellular domains (ECDs) of several mGluRs have been determined, the calcium-binding site(s) and structural determinants of Ca^{2+}-modulated signaling in the Glu receptor family remain elusive. Here, we identify a novel Ca^{2+}-binding site in the mGluR1α ECD using a recently developed computational algorithm. This predicted site (comprising Asp-318, Glu-325, and Asp-322 and the carboxylate side chain of the receptor agonist, Glu) is situated in the hinge region in the ECD of mGluR1α adjacent to the reported Glu-binding site, with Asp-318 involved in both Glu and calcium binding. Mutagenesis studies indicated that binding of Glu and Ca^{2+} to their distinct but partially overlapping binding sites synergistically modulated mGluR1α activation of intracellular Ca^{2+} ($[Ca^{2+}]_i$) signaling. Mutating the Glu-binding site completely abolished Glu signaling while leaving its Ca^{2+}-sensing capability largely intact. Mutating the predicted Ca^{2+}-binding residues abolished or significantly reduced the sensitivity of mGluR1α not only to $[Ca^{2+}]_o$ and $[Gd^{3+}]_o$ but also, in some cases, to Glu. The dual activation of mGluR1α by $[Ca^{2+}]_o$ and Glu has important implications for the activation of other mGluR subtypes and related receptors. It also opens up new avenues for developing allosteric modulators of mGluR function that target specific human diseases.

Metabotropic glutamate receptors (mGluRs)[2] have key functions in a variety of different neurological processes, including memory, learning, pain, synaptic plasticity, and the control of the activity of various circuits throughout the brain (1). The mGluRs belong to family C of the large superfamily of G protein-coupled receptors (GPCRs). Family C GPCRs (also referred to as family 3 GPCRs, the nomenclature that will be utilized here) also include the Ca^{2+}-sensing receptor (CaSR), $GABA_B$ receptors, taste receptors, and putative pheromone receptors (2). All members of the family 3 GPCRs share similar domain architecture, including venus flytrap-like extracellular domains (ECD), heptahelical transmembrane domains, and intracellular C-terminal C-tails. The mGluRs fall into three groups and eight subtypes. Group I comprises mGluR1 and mGluR5 (3). mGluR1 is expressed mainly around a core of ionotropic glutamate receptors in the postsynaptic densities of neurons and functions as a disulfide-linked homodimer (4). Upon activation by its agonists, the intracellular domains of the group I mGluRs associate with the G protein $G_{q/11}$ to activate phospholipase C, which subsequently converts phosphatidylinositol bisphosphate (PIP_2) to diacylglycerol and inositol trisphosphate (IP_3), thereby releasing Ca^{2+} from the endoplasmic reticulum, as well as activating protein kinase C (PKC) and other downstream effectors (5).

The issues of whether mGluRs respond to extracellular calcium ($[Ca^{2+}]_o$) and how calcium binding modulates the family 3 GPCRs have attracted extensive investigation. On the basis of sequence homology to CaSR, mGluRs were postulated to be capable of responding to $[Ca^{2+}]_o$. $[Ca^{2+}]_o$ has been proposed to either activate mGluR1 directly or to act as a positive mGluR1 modulator (6, 7). Kubo *et al.* (6, 8) reported that $[Ca^{2+}]_o$, as well as Glu, can trigger intracellular responses elicited by mGluR1, mGluR3, and mGluR5. $[Ca^{2+}]_o$ or Gd^{3+} further stimulate the activity of mGluR1α even after saturation of the Glu response and vice versa (6). In addition, mGluR1α responds to 5 mM $[Ca^{2+}]_o$ in Purkinje cells prepared from global mGluR1α knock-out mice in which the receptor has been specifically knocked into Purkinje cells, whereas the Purkinje cells from the mGluR1α global knock-out mice themselves cannot sense $[Ca^{2+}]_o$ (9, 10). On the basis of these studies, $[Ca^{2+}]_o$ is postulated to mediate postsynaptic efficacy through it action on mGluR1 (11). Moreover, Glu triggers $[Ca^{2+}]_i$ oscillations in a manner that is modulated by $[Ca^{2+}]_o$ (12), as R, 5-3, 5-Dihy-

* This work was supported, in whole or in part, by National Institutes of Health Grants GM081749-01 (to J. J. Y.), DK078331 (to E. M. B.), and NS055179 (to R. A. H.).

[S] The on-line version of this article (available at http://www.jbc.org) contains supplemental "Experimental Procedures," "Results," Figs. S1 and S2, Tables S1 and S2, and references.

[1] To whom correspondence should be addressed: Dept. of Chemistry, Georgia State University, 552 Natural Science Center, Atlanta, GA 30303. Tel.: 404-413-5520; Fax: 404-413-5551; E-mail: chejjy@langate.gsu.edu.

[2] The abbreviations used are: mGluR, metabotropic glutamate receptor; GPCR, G protein-coupled receptor; CaSR, Ca^{2+}-sensing receptor; ECD, extracellular domain; $[Ca^{2+}]_o$, extracellular calcium; $[Ca^{2+}]_i$, intracellular calcium; PDB, Protein Data Bank; LRET, luminescence energy transfer.

droxylphenylglycine, an agonist of group I mGluRs, generated inward currents that were enhanced by $[Ca^{2+}]_o$ (10). In contrast, Nash *et al.* (13) concluded that mGluR1α is not a calcium-sensing receptor because its response to the agonist L-quisqualate is not sensitive to $[Ca^{2+}]_o$. However, the effect of $[Ca^{2+}]_o$ on the EC_{50} for quisqualate was not examined. Any putative Ca^{2+}-binding sites capable of regulating mGluR signaling remain "invisible" in six crystal structures of the ECD of mGluR1α determined to date (14, 15), as well as the ECDs and cysteine-rich domains of mGluR3 and mGluR7 (15, 16). One Gd^{3+} ion binds to mGluR1 between the helices of lobe 2 (LB2) at the dimer interface of the ECD, far from the Glu-binding site (14, 17). Removing the Gd^{3+}-binding residue, E238Q, eliminated sensitivity to Gd^{3+} but not sensitivity to $[Ca^{2+}]_o$ and Glu (17, 18). Two Gd^{3+} ions visible in the crystal structure were ignored by these authors, although one of them is located near the critical hinge region coordinated by Asp-322, Asp-324, and Asp-493 (14). This observation also suggests strongly that a Ca^{2+} ion could bind to this region of the protein. The invisibility of Ca^{2+}-binding sites in the x-ray structures of the mGluRs represents a major challenge shared among other Ca^{2+}-modulated proteins functioning at high Ca^{2+} concentrations, like those in the extracellular fluids, due to their low Ca^{2+}-binding affinities (K_d, ~0.1–1.5 mM) and irregular binding geometries (19). Our understanding of the role of Ca^{2+} as an extracellular signal acting via family 3 GPCRs beyond CaSR is severely hampered by the lack of adequate information about the location and properties of the Ca^{2+}-binding sites of this class of proteins.

We report herein the identification of a novel Ca^{2+}-binding site adjacent to the Glu-binding site in the hinge region of the ECD of mGluR1α (14, 15), which was found by using our recently developed the MUG (multiple geometries) algorithm (20–22). MUG is a graphic geometry-based Ca^{2+}-binding site prediction software. It extracts oxygen clusters from Protein Data Bank (PDB) files and assumes a Ca^{2+} center for each cluster. The clusters then are verified by setting parameters for geometric filters that define the range of distance between oxygen atoms and Ca^{2+}. The clusters satisfying the parameter setting were considered candidates for Ca^{2+}-binding pockets. The putative Ca^{2+}-binding pockets of lower quality were further modified by allowing rotation of the side chains of predicted liganding residues. To investigate a single Ca^{2+}-binding site present within a short stretch of amino acids, normally less than 30 residues, we engineered the short loop into a scaffold protein, CD2. Intact CD2 does not bind Ca^{2+} and is tolerant of site-directed mutagenesis without undergoing changes in its overall structure. Then the metal-binding capabilities of the key predicted Ca^{2+}-binding residues were further characterized using luminescence energy transfer (LRET) and site-directed mutagenesis (23, 24). Finally, we investigated the intracellular Ca^{2+} responses resulting from the binding of $[Ca^{2+}]_o$, $[Gd^{3+}]_o$, or Glu individually or of both $[Ca^{2+}]_o$ and Glu together by expressing wild type and mGluR1α variants with predicted ligand residues mutated. Our studies suggest that Asp-318, Asp-322, and Glu-325 at the predicted site are involved in Ca^{2+} binding and that mutation at Asp-318 and Glu-325 also abolishes responsiveness of the receptor to $[Gd^{3+}]_o$. The ligands for Glu binding, in contrast, although also including Asp-318, are otherwise distinct (14, 15, 25). Notably, the carboxylate group of the side chain of Glu also contributes to the binding site for Ca^{2+}. We propose a dual activation mechanism whereby the simultaneous binding of Glu and Ca^{2+}, at their separate but partially overlapping binding sites, potentiates one another's actions to yield maximal activation of mGluR1α.

EXPERIMENTAL PROCEDURES

Computational Prediction of Ca^{2+}-binding Sites in mGluR1α and Molecular Modeling—The three-dimensional coordinates of the crystal structures of the ECD of mGluR1α were obtained from the PDB (PDB entry codes: 1EWT, 1EWK (15), and 1ISR (14)). Hydrogen atoms were added using the Sybyl7.2 package (Tripos Inc., St. Louis, MO). The identification of putative Ca^{2+}-binding sites in the ECD of mGluR1α was performed using MUG, a graph theory-based algorithm (21) developed by our laboratory. The Ca–O distance in the software was set to 1.6–3.1 Å with a set average cutoff of 2.4 Å (26, 27), and the O–O distance was set to 6.0 Å (21). Side chain atoms were rotated to accommodate Ca^{2+}-induced local conformational changes (48). Furthermore, electrostatic surface potential maps were constructed using Delphi (28), and GRASP (29) was then used to render and modify the image. The linear, putative Ca^{2+}-binding site was added into the scaffold protein CD2 between Ser-52 and Gly-53 with triple Gly linkers at both ends, and the combined grafting model was generated by Modeler 9v4 (30).

Plasmid, Expression, and Purification of Proteins—The predicted linear Ca^{2+}-binding site, termed mGluR1-1, resides between Gly-316 and Gly-337 (GSDGWADRDEVIEGYEVEANGG). This sequence, grafted into CD2 between Ser-52 and Gly-53 in the plasmid pGEX-2T-CD2 (31), was named CD2.D1. The engineered protein was expressed as a GST fusion protein and purified using GS4B resin as described (32). Site-directed mutagenesis was performed using the multisite-directed mutagenesis kit (Stratagene, Cedar Creek, TX).

Tb^{3+} Titration and Ca^{2+} Competition—In Trp-sensitized Tb^{3+}-LRET experiments, emission spectra from 500 to 580 nm were recorded with excitation set at 282 nm; slit widths were set at 8 nm for excitation and 12 nm for emission. A glass filter with a cutoff of 320 nm was utilized to circumvent secondary Rayleigh scattering. Tb^{3+} titration and metal competition assays were performed as described previously (24). 500 mM K^+, 10 μM La^{3+}, 10 μM Gd^{3+}, 1 mM Mg^{2+}, and 1 mM Ca^{2+}, respectively, was used to selectively compete with Tb^{3+}. Each experiment was carried out independently in triplicate.

Quantitatively Determined Membrane Expression of the mGluR1α Mutants Using Flow Cytometry—PcDNA-mGluR1α (donated by Dr. Randy Hall's laboratory) contained a FLAG tag at the N terminus of the receptor, and mCherry was genetically fused to the C terminus with a linker, GGNSGG. After 2 days of transient expression of mGluR1α and its mutants (D318I, D322I, E325I, and N335I) in HEK293 cells grown on polylysine-coated dishes, cells were incubated in 1× phosphate-buffered saline (PBS) supplemented with 1/1000 anti-FLAG and 1/100 fetal bovine serum (FBS) at 4 °C. The cells were then washed three times with 1× Tris-buffered saline (TBS) and fixed using 4% formaldehyde at room temperature for 15 min. After being washed three times with 1× TBS, the receptors on the cell sur-

face were then labeled with Alexa Fluor® 488 goat anti-mouse IgG (Invitrogen) for 30 min at 37 °C. The cells were then collected in 1× PBS, and the intensity of green and red fluorescence was measured using LSRFortessa (BD Biosciences). The ratios of green and red fluorescence from mGluR1α and the mutated receptors were normalized to the amount of receptors expressing on the cell surface relative to total receptors (total cellular expression of receptor). Data were collected from three dishes.

Measurement of $[Ca^{2+}]_i$ Responses of mGluR1α and Its Mutants with or without $[Ca^{2+}]_o$ or Glu—Measurement of $[Ca^{2+}]_i$ was performed as described (24). In brief, wild type mGluR1α and its mutants (D318I, D322I, D324I, E325I, and E328I) were transiently transfected into HEK293 cells and cultured for 2 additional days. The cells on the coverslips were subsequently loaded using 4 μM Fura-2 AM in 2 ml of physiological saline buffer (10 mM HEPES, 140 mM NaCl, 5 mM KCl, 0.55 mM $MgCl_2$, and 1 mM $CaCl_2$, pH 7.4). The coverslips were mounted in a bathing chamber on the stage of a fluorescence microscope. Fura-2 emission signals from single cells excited at 340 or 380 nm were collected utilizing a Leica DM6000 fluorescence microscope in real time as the concentration of extracellular Ca^{2+} was increased in a stepwise manner. The ratio of emitted fluorescence at 510 nm resulting from excitation at 340 or 380 nm was further analyzed to obtain the intracellular Ca^{2+} response as a function of changes in $[Ca^{2+}]_o$. Then, the sensitivity of mGluR1α and its mutants (D322I, D324I, E325I, and E328I) to extracellular glutamate was measured by increasing the extracellular glutamate concentration in the presence of 1.8 mM Ca^{2+}. The glutamate concentrations at which the intracellular Ca^{2+} responses of mGluR1α and its mutants were first observed and, subsequently, saturated were determined. Moreover, to further characterize the influence of $[Ca^{2+}]_o$ to Glu-induced $[Ca^{2+}]_i$ release through wild type mGluR1α, an additional 5 or 10 mM Ca^{2+} was added to the perfusate. $[Ca^{2+}]_i$ was measured as described above during changes in $[Ca^{2+}]_o$ and/or Glu.

Measurement of Intracellular Ca^{2+} Release Mediated by mGluR1α and Its Mutants in the Presence of Extracellular Gd^{3+}—Changes in $[Ca^{2+}]_i$ in response to the addition of Gd^{3+} were determined as just described. Specifically, cells were incubated in incubation buffer (140 mM NaCl, 4 mM KOH, 10 mM HEPES, 1.5 mM $CaCl_2$, 1 mM $MgCl_2$, 10 mM glucose, pH 7.4) for up to 1.5 h, and Gd^{3+} (made up in 140 mM NaCl, 4 mM KOH, 10 mM HEPES, and 0.3 mM $MgCl_2$, pH 7.4) was added at the concentrations described under "Results." The $[Ca^{2+}]_i$ responses of mGluR1α after the introduction of mutations in the Glu-binding site were measured similarly.

Data Analysis and Curve Fitting—At each agonist concentration, all of the transfected cells in the microscopic field from three independent experiments were selected for analysis, and at least 60% of the cells displaying normal responses were analyzed. The cells that did not respond to the agonists or displayed a sigmoidal curve with a stable plateau after treatment with high $[Ca^{2+}]_o$ were excluded. These latter cells maintained a constant, high plateau of the intracellular Ca^{2+} concentration, perhaps because the plasma membrane was excessively permeable to Ca^{2+}. To normalize the concentration response curves for the responses to $[Ca^{2+}]_o$, the maximal response of wild type

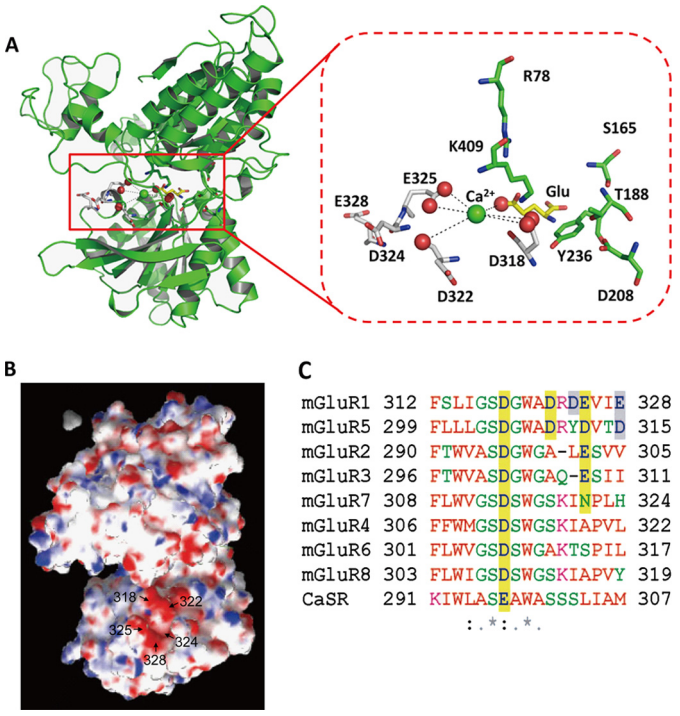

FIGURE 1. **Predicted Ca^{2+}-binding pocket in ECD of mGluR1α.** *A*, location of the predicted Ca^{2+}-binding site in the ECD (PDB entry code: 1EWK). The proposed key residues are indicated and highlighted in *red* (model generated by PyMOL). *B*, electrostatic potential map of ECD. The predicted Ca^{2+}-binding site is in the hinge region and shares residue Asp-318 with the Glu-binding site. *C*, alignment of the grafted fragment in mGluRs and CaSR. Asp-318 is conserved in all of the receptors; Glu-325 is conserved in group I and II mGluRs; Asp-322 is conserved in group I mGluRs.

mGluR1α to extracellular Glu was set at 100% so that the maximal responses of mutant receptors to $[Ca^{2+}]_o$ or Glu were transformed into percentages relative to the response of WT mGluR1α to Glu. Data were fitted using the Hill equation as described previously (23).

RESULTS

Prediction of a Novel Ca^{2+}-binding Site Adjacent to the Glu-binding Site in the ECD of mGluR1α—We recently developed the computational algorithm MUG, which predicts Ca^{2+}-binding sites using graph theory by identifying all possible liganding oxygen clusters and finding maximal cliques. The positions of Ca^{2+} and its liganding groups in 144 calcium-binding proteins can be predicted with 0.22–0.49 Å accuracy by geometric filters established on the basis of an extensive survey of known Ca^{2+}-binding sites in the Protein Data Bank (19). To accommodate Ca^{2+}-induced conformational changes, the side chains of putative Ca^{2+}-binding ligand residues were subjected to rotation using a rotamer library (MUG^{SR}) (48). Fig. 1 shows one predicted Ca^{2+}-binding site identified here in the crystal structure of the mGluR1α ECD (PDB entry code: 1EWK) using the MUG algorithm. Two other predicted sites not included in this report were also revealed by MUG, one of them (site 2) residing in the Mg^{2+}-binding pocket (Leu-86—Gly-102) inferred from the crystal structure and the other one located within a long loop (Asp-125—Lys-153) that was invisible in the crystal structure because of its high flexibility and was repaired using Modeler (30). The third predicted Ca^{2+}-binding site (site 3), encompassing Ser-129 to Gly-144, was present within this missing loop.

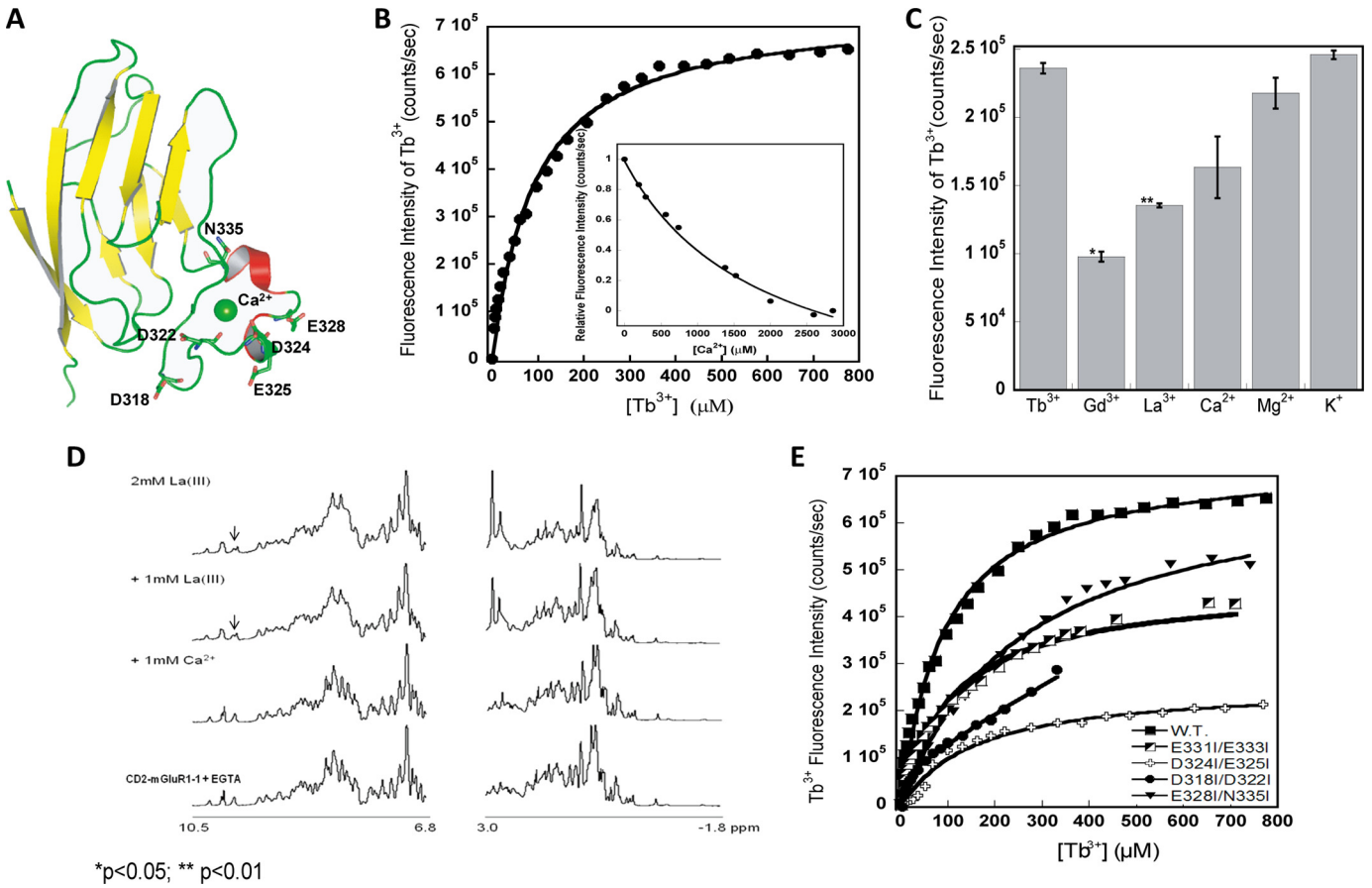

FIGURE 2. **Metal binding properties of the grafted Ca^{2+}-binding site.** *A*, three-dimensional illustration of the modeled structure of the engineered protein CD2.D1, based on the crystal structures of CD2 (PDB entry code: 1HNG (35)) and the mGluR1α ECD (PDB entry code: 1EWT (8)). *B*, Tb^{3+} titration and Ca^{2+} competition (shown as *inset*) of CD2.D1. The engineered protein bound Tb^{3+} and Ca^{2+} with dissociation constants of 49 ± 9 μM and 1.8 ± 0.1 mM, respectively. Substitution of putative metal-binding ligand residues with Ile decreases Tb^{3+} binding affinity. Tb^{3+} binding curves of a series of CD2-mGluR1 double mutants, E331I/E333I, D324I/E325I, D318I/D322I, and E328I/N335I. All measurements were carried out in a buffer containing 20 mM PIPES and 10 mM KCl, pH 6.8. *C*, Tb^{3+} binding curves of a series of CD2-mGluR1 double mutants: CD2.D1-1 (E331I/E333I), CD2.D1-2 (D324I/E325I), CD2.D1-3 (D318I/D322I), and CD2.D1-4 (E328I/N335I). All of the measurements were carried out in a buffer containing 20 mM PIPES and 10 mM KCl, pH 6.8. D318I/D322I obviously decreased Tb^{3+} binding affinity, whereas D324I/E325I displays two phases. The Tb^{3+} binding affinity of the engineered protein was clearly impaired by these two pair of mutations ($n = 3$). *D*, La^{3+} binding to the engineered protein CD2.D1 monitored by $^1D^1H$ NMR. 1 or 2 mM La^{3+} results in the peak split at the aromatic group region. *E*, metal selectivity of CD2.D1. The addition of 500 mM K^+, 1 mM Ca^{2+}, 1 mM Mg^{2+}, 100 μM Gd^{3+}, or 100 μM La^{3+} to the pre-equilibrated Tb^{3+} (30 μM) and protein (3 μM) solution was carried out independently. The resultant changes in the Tb^{3+} luminescence signal were monitored at 545 nm (*, $p < 0.05$; **, $p < 0.01$).

The predicted Ca^{2+}-binding site studied in detail here comprises the carboxyl side chains of Asp-318 and Glu-325, the main chain carbonyl Asp-322 in a flexible loop of mGluR1α, and the carboxyl side chain of Glu-701 (a ligand for glutamate). This predicted Ca^{2+}-binding site is located at the hinge region in the ECD adjacent to the reported Glu-binding site (Arg-74, Ser-165, Thr-188, Asp-208, Tyr-236, Asp-318, and Lys-409) (15, 25), with Asp-318 predicted to be involved in both Glu and Ca^{2+} binding. Thus, Ca^{2+} and Glu, when bound to the receptor, both bind to Asp-318. Asp-318 and Asp-322 can be identified in the Glu-free form (PDB entry code: 1EWT), whereas the direct binding of Ca^{2+} to the carboxyl side chain of the agonist Glu-701 is visualized only in the Glu-loaded form (PDB entry code: 1EWK). Thus, the agonist Glu provides an additional ligand for Ca^{2+} when the former is bound to the receptor, which is very different from intracellular Ca^{2+}-binding trigger proteins such as calmodulin that lack any additional chelating groups from molecules other than the residues within the Ca^{2+}-binding protein itself, except for water. Fig. 1*B* shows that the predicted Ca^{2+}-binding pocket has a highly negatively charged surface as revealed by Delphi in the structures of three solved forms of the ECD within mGluR1α (Fig. 1*B*).

Obtaining Site-specific Ca^{2+}/Ln^{3+}-binding Affinities by a Grafting Approach—To probe the Ca^{2+}-binding capability of the predicted Ca^{2+}-binding site in mGluR1α, we utilized our grafting approach by inserting the protein sequence encompassing the putative mGluR1α Ca^{2+}-binding site into the host protein, CD2.D1 (denoted as CD2-mGluR1-1). The inserted sequence contains all predicted Ca^{2+}-binding residues except Glu-701. This approach had previously enabled us to obtain site-specific Ca^{2+} binding affinities of the EF-hand motifs from calmodulin and linear Ca^{2+} binding sequences, free from the limitations of working with membrane proteins (32, 33). The putative mGluR1α Ca^{2+}-binding site was flanked by flexible triple-Gly linkers and inserted between Ser-52 and Gly-53 of CD2.D1 (Fig. 2*A*) to ensure a native-like conformation and close proximity (<15~20 Å) to Trp-32 in order to enhance the Tb^{3+}-LRET signal. Indeed, grafting the putative Ca^{2+}-binding loop from mGluR1α did not significantly change the secondary and tertiary structures of CD2, as revealed by circular

TABLE 1
Tb^{3+} binding affinities of the engineered protein CD2.D1 and its double mutants ($n = 3$)

Proteins	Mutations	Dissociation constant (K_d)
CD2.D1	WT	49 ± 9 μM (Ca^{2+}, 1.8 ± 0.1 mM)
CD2.D1-1	E331/E333I	85 ± 18 μM*
CD2.D1-2	D324/E325I	113 ± 5 μM
CD2.D1-3	D318/D322I	>4.8 mM*
CD2.D1-4	E328/N335I	299 ± 15 μM*

*, $p < 0.05$.

dichroism, Trp fluorescence, and NMR chemical shifts (supplemental Fig. S1). Fig. 2*B* shows that Tb^{3+} (which has the same coordination chemistry as Ca^{2+}) elicits an increase in fluorescence of CD2.D1 at 550 nm when excited at 280 nm due to Tb^{3+}- LRET. CD2.D1 had a Tb^{3+} binding affinity of 49 ± 9 μM (Fig. 2*B* and Table 1). Ca^{2+} displaced bound Tb^{3+} (Fig. 2*B*), thereby decreasing the Tb^{3+}-LRET signal. CD2.D1 has a Ca^{2+} dissociation constant of 1.80 ± 0.12 mM determined in this manner (Table 1).

Because mGluR1α is modulated by various polyvalent cations, including Ca^{2+}, Gd^{3+}, Tb^{3+}, La^{3+}, Mn^{2+}, and Mg^{2+} (6), we tested the metal binding selectivity of CD2.D1 by applying K^+, Mg^{2+}, La^{3+}, or Gd^{3+} to compete with prebound Tb^{3+}. Fig. 2*C* shows that the luminescence intensity of Tb^{3+} decreased significantly upon adding trivalent La^{3+} or Gd^{3+}, indicating that Tb^{3+} bound to the pocket was replaced by these metal ions. Gd^{3+} had the strongest capacity to displace Tb^{3+}. Similarly, adding La^{3+} to CD2.D1 produced a split in the resonance of CD2.D1 at 10 ppm (Fig. 2*D*). Ca^{2+} competed more effectively than Mg^{2+}, whereas K^+ failed to compete with Tb^{3+}.

Next, we utilized mutagenesis studies to examine the contribution of proposed ligand-binding residues to metal-binding capability. Double substitutions of negatively charged residues by Ile to delete negative charges but preserve bulky side chains in the proposed binding pocket, as seen in the mutants D324I/E325I, D318I/D322I, and E328I/N335I, produced 2.3-, 6.1-, or 98-fold increases in the respective dissociation constant values (Fig. 2, *B* and *E*). However, removing the negative charges from the non-Ca^{2+}-binding residues, Glu-331 and Glu-333 (E331I/E333I) (Fig. 2, *B* and *E*) produced a less than 2-fold change in the K_d, with a modest alteration in Tb^{3+} binding to the predicted binding pocket.

Membrane Expression of mGluR1α and Its Mutants—WT mGluR1α and its mutant forms (D318I, D322I, and E325I) were expressed heterogeneously in HEK293 cells. The receptors expressed on the cell membrane were visualized by confocal microscopy (supplemental Fig. S2) and flow cytometry (Fig. 3). Supplemental Fig. S2 shows that the mutations did not affect the distribution of the receptors on the membrane. We calculated the ratio of intensities of green and red fluorescence measured using flow cytometry (LSRFortessa, BD Biosciences); the mutant receptors displayed expression levels on the cell membrane comparable with that of the wild type receptor, although E325I displayed a somewhat lower membrane expression level (Fig. 3; $n = 3$). Thus, the mutations involving the predicted Ca^{2+}-binding site had little effect on the surface expression of the respective mutant receptors.

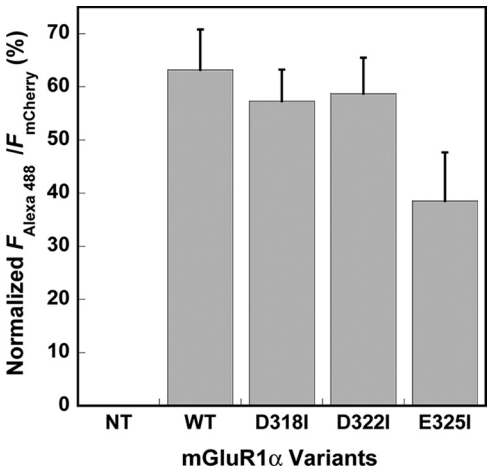

FIGURE 3. **Surface expression of WT mGluR1α and its mutants.** mGluR1α carries FLAG tag at its N terminus and mCherry at its C terminus. mGluR1α and its mutants were transiently expressed in HEK293 cells seeded on 50-mm dishes coated with polylysine. After incubation with anti-FLAG, the receptors on the membrane could be visualized using a secondary antibody, Alexa 488-anti-mouse IgG (Invitrogen). Emissions at 520 and 610 nm were collected by flow cytometry (LSRFortessa, BD Biosciences); these represent receptors present on the cell membrane and overall, respectively. Ratios of fluorescence at 520–610 nm indicate the membrane expression levels of WT mGluR1α and its mutants. Emission at 520 nm (green signal) reflects the membrane expressed receptors, whereas the red signal at 610 nm from mCherry is a measure of total expression of the receptor. *NT* indicates non-transfected cells, which display no fluorescence. Although E325I displays a relatively lower surface expression, the other mutants have membrane expression level comparable with that of WT mGluR1α ($n = 3$).

Extracellular Ca^{2+} Triggers mGluR1α-mediated Intracellular Responses—We next examined the mGluR-mediated intracellular Ca^{2+} responses in HEK293 cells transfected with mGluR1α-mCherry. The fluorescent protein mCherry was fused to mGluR1α to correlate cellular responses with the expression of mGluR1α. We chose HEK293 cells as a model because this cell line lacks endogenous mGluR1α (34). mGluR1α-mCherry was well expressed and correctly targeted to the cell membrane (Figs. 3 and 4*A* and supplemental Fig. S2), and Fura-2 was efficiently loaded (Fig. 4*B*). Single cell, real time imaging was performed using fluorescence microscopy. To minimize receptor desensitization by agonists, the responses to each concentration of added Ca^{2+} or Glu were examined using separate coverslips.

In the absence of exogenous Glu, the addition of $[Ca^{2+}]_o$ at less than 1.8 mM did not induce any $[Ca^{2+}]_i$ response in HEK293 cells transfected with WT mGluR1α. Adding ≥3.0 mM Ca^{2+} to the medium elicited a transient $[Ca^{2+}]_i$ increase followed by a long lasting plateau (Fig. 4*C*); this response was maximal at ≥5.0 mM $[Ca^{2+}]_o$, with an EC_{50} of 3.0 mM. Furthermore, adding 0.5 or 30 μM Glu significantly enhanced the maximal response of mGluR1α to $[Ca^{2+}]_o$ by 1.3- and 1.7-fold, respectively (Fig. 5). The EC_{50} value for $[Ca^{2+}]_o$ decreased from 3.0 to 2.8 and 0.1 mM, respectively (Fig. 5 and Table 2).

The response of wild type mGluR1α to Glu was investigated in physiological saline buffer with 1.8 mM Ca^{2+}. Wild type mGluR1α only responded at ≥0.5 μM Glu, and this response was saturated at 30 μM Glu. Fig. 6*A* shows that at 1.8 mM Ca^{2+}, the addition of >30 μM Glu evoked large $[Ca^{2+}]_i$ responses.

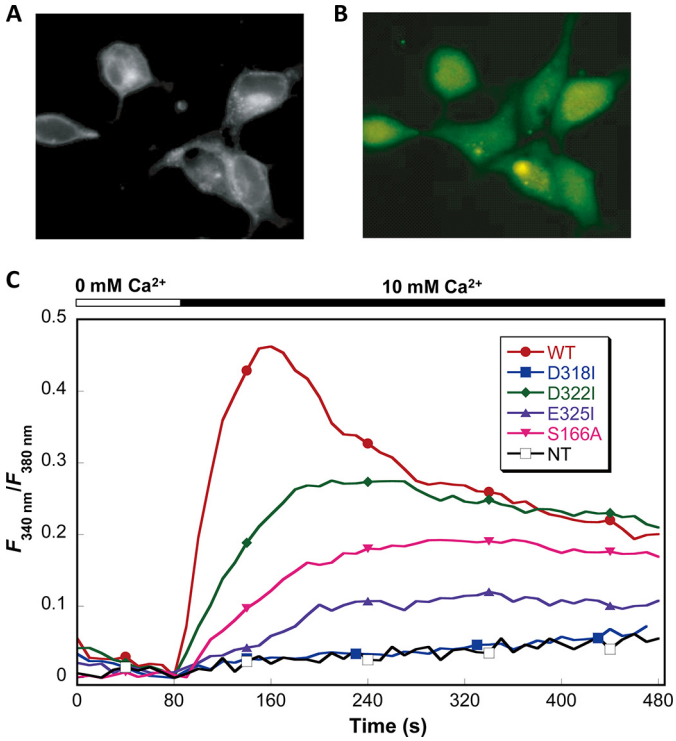

FIGURE 4. **Intracellular Ca^{2+} response of WT mGluR1α and its mutants.** WT mGluR1α and D318I-mGluR1α were overexpressed in HEK293 cells. Fura-2 was then loaded into the cells, and the $[Ca^{2+}]_i$ level was measured by monitoring emission at 510 nm with excitation at 340 or 380 nm. *A*, *red* fluorescence of mCherry on the C terminus of mGluR1α indicates the presence of the receptor or its mutants. *B*, cells were loaded with Fura-2-AM to measure $[Ca^{2+}]_i$ level. *C*, $[Ca^{2+}]_i$ release triggered by $[Ca^{2+}]_o$ in WT mGluR1α and its mutants. D318I and E325I eliminate the $[Ca^{2+}]_i$ response, whereas D322I and S166A reduce it. *NT*, non-transfected cells.

However, when $[Ca^{2+}]_o$ was reduced from 1.8 mM to close to zero (no Ca^{2+} added to the medium), 30 μM Glu still activated mGluR1α (Fig. 5). There was, however, a reduced maximal response (29%) (Fig. 5), possibly because of the depletion of intracellular calcium stores. This result suggests that Glu triggers the activation of mGluR1α and that this effect can be enhanced by $[Ca^{2+}]_o$.

To study the synergy of $[Ca^{2+}]_o$ and Glu binding to mGluR1α, the combination indices for quantitative evaluation of synergism were calculated using Calcusyn (35). With 0.5 or 30 μM Glu, the combination indices were <1 when $[Ca^{2+}]_o$ reached a physiological level (>0.5 mM) (supplemental Table S2), suggesting that Glu and Ca^{2+} synergistically modulate mGluR1α-mediated signaling.

Effects of $[Ca^{2+}]_o$ on Glu-induced $[Ca^{2+}]_i$ Release by Wild Type mGluR1α—To determine the role of $[Ca^{2+}]_o$ on Glu-mediated activation of wild type mGluR1α. 5 and 10 mM $[Ca^{2+}]_o$ were added to the perfusion system in addition to the 1.8 mM already present in the perfusate. As shown in Fig. 7, compared with the response in 1.8 mM $[Ca^{2+}]_o$, both 5 and 10 mM $[Ca^{2+}]_o$ enhanced the responses of WT mGluR1α to Glu by reducing the EC_{50} values from 1.7 to 0.9 and 0.4 μM, respectively (Table 2), although the maximal responses remained comparable with those at 1.8 mM $[Ca^{2+}]_o$. This indicates that $[Ca^{2+}]_o$ potentiates the sensitivity of mGluR1α to Glu and that this effect increases at higher levels of $[Ca^{2+}]_o$.

Effects of Mutating Proposed Ca^{2+}-binding Residues on $[Ca^{2+}]_o$- or Glu-evoked $[Ca^{2+}]_i$ Responses—To further understand the potential physiological role of this proposed Ca^{2+}-binding site, we compared the mGluR-mediated $[Ca^{2+}]_i$ responses in HEK293 cells transfected with the WT or mutated versions of mGluR1α. Fig. 4*C* shows that without Glu, substituting the predicted Ca^{2+}-binding residues Asp-318 and Glu-325 with Ile eliminates the transient $[Ca^{2+}]_i$ response toward $[Ca^{2+}]_o$. In addition, the mutation D322I also reduced the transient $[Ca^{2+}]_i$ response by 16–20% while increasing the EC_{50} from 3.0 mM $[Ca^{2+}]_o$ for the wild type receptor to 4.2 mM for D322I (Fig. 5 and Table 2), although all mutants were expressed at levels comparable with the WT receptor, as assessed by immunofluorescence and flow cytometry (Fig. 3 and supplemental Fig. S2). These results suggest that the predicted Ca^{2+}-binding residues, Asp-318, Glu-325, and Asp-322 (especially the first two), are important for the sensitivity of mGluR1α to modulation by $[Ca^{2+}]_o$. However, S166A maintains Ca^{2+} sensitivity with a lower maximal response (Fig. 4*C*), although Ser-166 was previously reported to be a potential Ca^{2+}-binding residue (6).

Effects of Mutating Predicted Ca^{2+}-binding Residues on Glu-potentiated $[Ca^{2+}]_i$ Responses—The Ca^{2+}-binding site identified here is adjacent to the previously defined Glu-binding site (Arg-78, Ser-165, Thr-188, Asp-208, Tyr-236, Asp-318, and Lys-409) (15, 25) (Fig. 1*B*). Asp-318 is the lone residue used in both the Glu- and Ca^{2+}-binding sites. Figs. 4 and 6 show that the mutation D318I completely eliminates the $[Ca^{2+}]_i$ response of mGluR1α to both $[Ca^{2+}]_o$ and Glu, even at concentrations of the latter as high as 30 μM. In contrast, the mutant E325I completely abolishes $[Ca^{2+}]_o$-mediated $[Ca^{2+}]_i$ responses without the agonist Glu (Figs. 4*C* and 5 and Table 2) but retains Glu-mediated $[Ca^{2+}]_i$ responses (Fig. 6*A*). However, its EC_{50} value for Glu-mediated responses is increased by ~18-fold (Fig. 6*B* and Table 2). These results further confirm that Glu-325 contributes to Ca^{2+} binding without directly liganding Glu (as shown by earlier studies of the binding site for Glu, which did not identify Glu-325 as a Glu ligand). However, the proximity of the Ca^{2+}- and Glu-binding sites may produce indirect, conformational effects of mutating residue 325 on Glu binding. Furthermore, D322I exhibited a reduction in EC_{50} for $[Ca^{2+}]_o$ by only 33%, consistent with it making a relatively minor contribution as a ligand for Ca^{2+} binding. In contrast to the marked impact of D318I and E325I on the EC_{50} for $[Ca^{2+}]_o$, removal of other charged residues, such as D324I and E328I, did not alter either the EC_{50} (3 and 8% changes, respectively) or the magnitude of the response to $[Ca^{2+}]_o$ significantly in the absence of Glu (104 ± 10 and 102 ± 5, respectively, of the control level) (Fig. 5 and Table 2).

Effect of Mutating Glu-binding Site on $[Ca^{2+}]_i$ Responses to Glu and Ca^{2+}—To further explore the synergistic interaction between the predicted Ca^{2+}- and Glu-binding sites, four mutations at Glu ligand residues (S165A, T188A, D208I, and Y236F) were generated. Consistent with studies reported previously (25), T188A and D208I entirely eliminated Glu sensitivity, whereas S165A and Y236F could be activated only by high concentrations (100 μM) of Glu (Fig. 8*A*). Interestingly, all receptors with mutated Glu-binding ligand residues (exception for

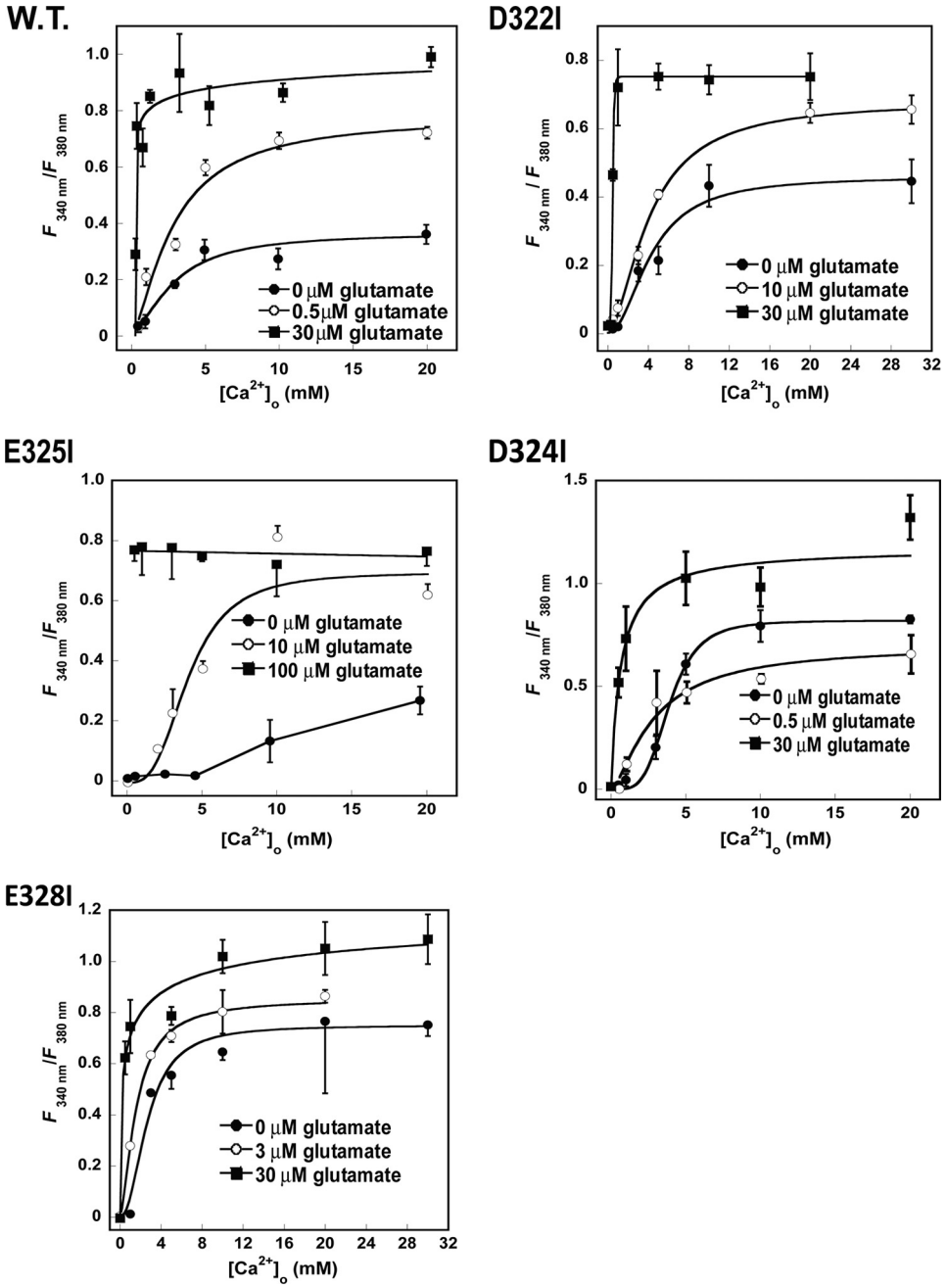

FIGURE 5. **Intracellular Ca^{2+} responses of WT mGluR1α and its mutants (D322I-mGluR1α, D324I-mGluR1α, E325I-mGluR1α, and E328I-mGluR1α) to $[Ca^{2+}]_o$ in the presence of Glu.** Shown are the additional Glu-enhanced responses of WT mGluR1α and all of its mutants to $[Ca^{2+}]_o$. The Glu concentrations that were added were determined by the responses of the wild type receptor or its mutants to Glu. That is, the Glu concentrations that evoked initial activation of or saturated the receptors were utilized for the $[Ca^{2+}]_o$-induced responses of the wild type receptor and its mutants. $[Ca^{2+}]_i$ levels were measured by the same methods described above. Notably, E325I loses sensitivity to $[Ca^{2+}]_o$ but can still sense $[Glu]_o$. However, its responsiveness to $[Ca^{2+}]_o$ in the presence of high concentration $[Glu]_o$ was not affected by increasing $[Ca^{2+}]_o$ ($n = 3$).

Asp-318) retained a sensitivity to $[Ca^{2+}]_o$ (Fig. 8*B* and Table 3), although their EC_{50} values were increased compared with that of wild type mGluR1α (Table 3), again perhaps owing to local conformational effects of mutating the Glu-binding site on Ca^{2+} binding. S165A and D208I increased the EC_{50} of the wild type receptor for $[Ca^{2+}]_o$ from 3.0 to 8.1 and 4.6 mM, respectively, although their maximal responses were comparable to that of the wild type receptor (Fig. 8*B* and Table 3). Conversely, T188A and D208I exhibited much reduced maximal responses (26 and 66%, respectively), whereas their EC_{50} values were comparable with that of the wild type receptor (Table 3). Taken together, these data show that it is possible to generate mGluR1α variants responding to either Glu or to Ca^{2+} alone. Thus mGluR1α can function as a true $[Ca^{2+}]_o$-sensing receptor, as certain mutants, such as S165A and D208I, do not respond to Glu but maintain their Ca^{2+}-sensing capability with only a modest increase in the EC_{50} for $[Ca^{2+}]_o$.

Effects of Mutations in Predicted Ca^{2+}-binding Site on Gd^{3+}-induced $[Ca^{2+}]_i$ Responses—Gd^{3+} is also revealed at the hinge region in the Fourier map, where it shares residues Asp-322 and Asp-324 from the loop that contributes to Ca^{2+} binding (14). Because of the low resolution of this crystal structure (4 Å), the highly flexible loop that binds Gd^{3+} in the crystal structure, and the similarity of the binding geometries of Gd^{3+} and Ca^{2+}, these two cations probably share, at least in part, the same residues. To address this possibility, the responses to $[Gd^{3+}]_o$ of D318I and E325I were compared with that of the wild type receptor. Consistent with results reported by Abe *et al.* (17, 36), the dose-response profiles of wild type mGluR1α display a bell-shaped curve. However, the introduction of the mutation D318I or E325I completely eliminated the receptor sensitivity to $[Gd^{3+}]_o$ (Fig. 9).

DISCUSSION

We utilized the computational algorithm MUG (22) to predict a novel Ca^{2+}-binding site in mGluR1α adjacent to the Glu-binding site shown in Fig. 1. This predicted Ca^{2+}-binding site (comprising Asp-318, Glu-325, Asp-322, and the carboxylate side chain of Glu-701) does not completely overlap the Glu-binding site (15, 25). However, both sites include Asp-318, which our data suggest is involved in both Glu and Ca^{2+} binding. The metal-binding capability of the predicted Ca^{2+}-binding residues in mGluR1α was verified by a grafting approach. Like wild type mGluR1α, the predicted Ca^{2+}-binding site grafted in a scaffold protein (CD2) exhibited metal selectivity for Ca^{2+} and its trivalent analogs, Gd^{3+}, Tb^{3+}, and La^{3+}, in contrast to the physiological

TABLE 2
$[Ca^{2+}]_i$ responses of WT mGluR1α and its mutants to $[Ca^{2+}]_o$ and Glu ($n = 3$)

Variants	$[Ca^{2+}]_o$				Glu	
	Glu concentration	EC_{50}	n_{Hill}	Maximal response[a]	EC_{50}[b]	Maximal response[a]
	μM	mM		%	μM	%
WT	0	3.0	1.7	75 ± 3	1.7	100 ± 3
	0.5	2.8	1.4	109 ± 7	0.9[c]	108 ± 1[c]
	30	0.1	0.5	128 ± 6	0.4[d]	130 ± 8[d]
D318I	0	None	None	No response	None	No response
D322I	0	4.3	2.0	63 ± 2	13.2	111 ± 2
	10	4.1	1.7	86 ± 5		
	30	0.5	7.2	105 ± 3		
E325I	0	None	None	No response	30.5	146 ± 2
	10	4.3	2.3	89 ± 12		
	100	ND[e]	ND[e]	117 ± 3		
D324I	0	3.9	4.1	104 ± 10	0.3	117 ± 7
	0.5	2.9	1.8	144 ± 4		
	30	0.6	1.0	162 ± 6		
E328I	0	2.5	2.7	102 ± 5	1.2	107 ± 12
	3	1.6	1.5	135 ± 13		
	30	2.2	0.3	147 ± 3		

[a] The maximal responses are normalized to the maximal response of wild type mGluR1α to Glu.
[b] Glu dose response was performed in 1.8 mM Ca^{2+}.
[c] Experiments performed in 5 mM Ca^{2+}.
[d] Experiments perfomed in 10 mM Ca^{2+}.
[e] ND, not determined.

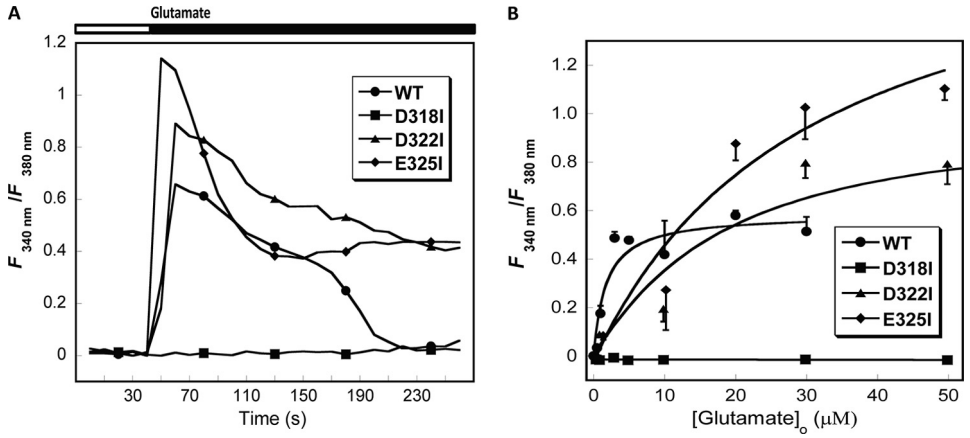

FIGURE 6. **Intracellular Ca^{2+} responses to extracellular Glu in HEK293 cells transfected with WT mGluR1α or its mutants.** Three negatively charged residues in the predicted Ca^{2+}-binding pocket (Asp-318, Asp-322, and Glu-325) were mutated into Ile. Along with WT mGluR1α, the mutants were transiently expressed in HEK293 cells. In the presence of 1.8 mM Ca^{2+}, extracellular Glu-induced intracellular Ca^{2+} release was measured by recording emission intensities at 510 nm excited at 340 and 380 nm, respectively. *A*, responses to Glu of mutations on Ca^{2+}-binding site. Except for mutant D318I, two other mutants, D322I, E325I, and WT mGluR1α display responsiveness to Glu. *B*, maximal response of WT mGluR1α and its mutants to Glu at a saturating concentration. Each single data point was performed in an individual dish, and the cells expressed mGluR1α showing responses to Glu were selected for analysis ($n = 3$).

monovalent cation, K^+, which exhibited no measurable affinity for the predicted site. The metal-binding capability of the predicted metal-binding ligand residues in mGluR1α was further verified by replacing negatively charged residues with Ile. The Ca^{2+} binding affinity of mGluR1α determined by the grafting approach (~1.8 mM) is within the physiological concentration of $[Ca^{2+}]_o$ in the nervous system (0.8–1.5 mM) (37), although this Ca^{2+} binding constant may be changed slightly *in vivo* by the local microenvironment and/or the presence of Glu released by nearby cells.

We further demonstrated that mGluR1α could be activated by either Glu or $[Ca^{2+}]_o$. Indeed, Glu and $[Ca^{2+}]_o$ act synergistically to elicit the maximal $[Ca^{2+}]_i$ responses observed here (Table 2). Mutating the Glu-binding site, such as T188A and D208I, in mGluR1α (Fig. 8*A* and Table 3), completely abolished the Glu-signaling capability of the receptor while leaving its Ca^{2+}-sensing capability largely intact, with only modest increases in EC_{50} for $[Ca^{2+}]_o$. These results suggest that mGluR1α can function as a true $[Ca^{2+}]_o$-sensing receptor, *i.e.* exhibiting robust activation by $[Ca^{2+}]_o$, in the absence of added Glu. Although we cannot rule out release of low concentrations of Glu by the HEK293 cells, it should be noted that some mutants of the receptor retained responsiveness to $[Ca^{2+}]_o$ despite complete loss of responsiveness to Glu. Moreover, even the addition of high exogenous concentrations of Glu failed to activate these mutants.

We have also shown that mutating predicted Ca^{2+}-binding residues abolishes or significantly not only reduces $[Ca^{2+}]_o$ sensitivity but also, in some cases, affects Glu-mediated responses. For example, E325I completely abolished $[Ca^{2+}]_o$-mediated $[Ca^{2+}]_i$ responses in the absence of Glu (Fig. 3*C* and Table 2). At the same time, this mutant retained sensitivity to Glu, albeit with an ~18-fold reduction in EC_{50} (without any decrease in maximal response) (Fig. 5 and Table 2). Thus, despite its not being a Glu-binding residue, the presence of an intact Ca^{2+}-binding ligand at Glu-325 considerably enhanced the affinity of mGluR1α for Glu. How could this take place? These results, in fact, are consistent with separate but overlapping Ca^{2+}- and Glu-binding sites (Figs. 1 and 10). As noted, positively charged Arg-323 is also very close to Ca^{2+} in the model, but it might not

affect Ca^{2+} binding because of the flexible backbone in the loop. Glu-325 is predicted to be a ligand for binding Ca^{2+} and not Glu. Glu-325 could be identified only in the x-ray structure of Glu-complexed mGluR1α (PDB entry code: 1EWK), indicating that 1) the binding of Glu could stabilize the side chain of Glu-325 in a conformation favorable for it to serve as a ligand for Ca^{2+} and/or 2) the bound Glu could then further enhance $[Ca^{2+}]_o$ binding by contributing an additional Ca^{2+}-binding ligand. Conversely, binding of Ca^{2+} to mGluR1α could increase the affinity of the Glu-binding site for its ligand by providing Ca^{2+} as an additional Glu ligand (Glu-701). Overall, mutating residues involved only in binding $[Ca^{2+}]_o$ (with the exception of Asp-318) had less dramatic effects than mutations at the Glu-binding site. Most of these mutants can be fully activated upon binding Glu, because the addition of high levels of Glu restores their EC_{50} and maximal responses to $[Ca^{2+}]_o$ to levels close to those of the wild type receptor. Additionally, a Gd^{3+} ion is also revealed in the crystal structure adjacent to the predicted Ca^{2+}-binding site, and it shares the same loop that contributes to Ca^{2+} binding. Mutations in the Ca^{2+}-binding residues in the loop, D318I and E325I, entirely eliminated Gd^{3+}-induced $[Ca^{2+}]_i$ release (Fig. 9). Although Glu-238, located at the interface of the two protomers, has been reported as a functional Gd^{3+} site, I120A, another mutation located at the interface of the receptor loses sensitivity to $[Ca^{2+}]_o$ (25). This indicates that the mutations at the interface of the two monomers cause markedly reduced activation of the receptor by either $[Gd^{3+}]_o$ or $[Ca^{2+}]_o$ and that the site at the hinge region is a true Gd^{3+}-binding site. This also highly suggests that our predicted Ca^{2+}-binding site can likewise bind Gd^{3+}.

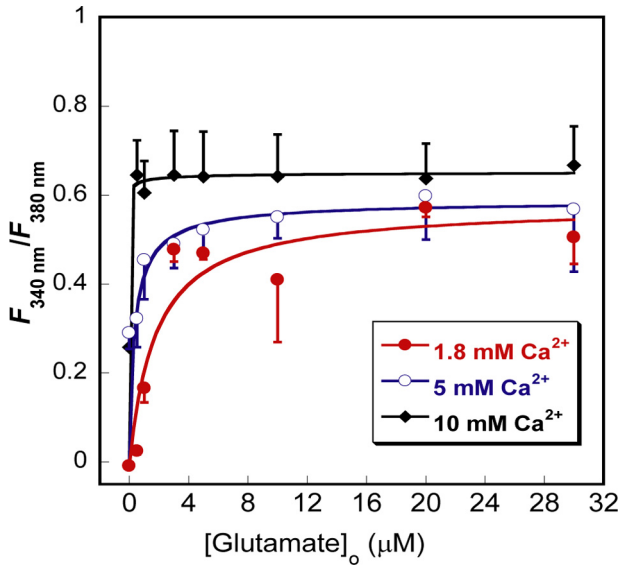

FIGURE 7. **Extracellular Ca^{2+} enhanced mGluR1α to sense extracellular Glu.** Responses of WT mGluR1α to extracellular Glu were assessed in buffers containing additional $[Ca^{2+}]_o$ (1.8, 5, and 10 mM). The maximal responses of the receptor to $[Glu]_o$ in 1.8, 5, and 10 mM $[Ca^{2+}]_o$ are comparable, but the EC_{50} values for the responses in the presence of 5 and 10 mM $[Ca^{2+}]_o$ are significantly decreased. Clearly, higher $[Ca^{2+}]_o$ reduces the EC_{50} of the receptor for $[Glu]_o$ ($n = 3$).

In view of these findings, we propose a working model of dual activation of mGluR1α by the two physiological activators, $[Ca^{2+}]_o$ and Glu, via their overlapping and interacting binding pockets at the hinge region of the ECD (Fig. 10). Increased concentrations of either Glu or $[Ca^{2+}]_o$ partially activate mGluR1α. However, full activation of mGluR1α with maximal sensitivity and maximal amplitude of the response to Glu requires simultaneous binding of both Glu and Ca^{2+}, with Asp-318 playing a key role in the synergy between the two agonists. In this sense, mGluR1α can be viewed as a "coincidence detector," requiring the binding of both ligands for maximal intracellular signaling.

Our proposed working model of mGluR1α is supported by previous studies from a number of groups working on both cultured cells and native brain tissue (6). Francesconi and Duvoisin (38) reported that mGluR1α in transfected cells is activated by $[Ca^{2+}]_o$ in the absence of Glu, indicating that mGluR1α is a Ca^{2+}-sensing receptor. Kubo *et al.* (6) showed that $[Ca^{2+}]_o$, as well as Glu, triggers intracellular responses in cultured cells and oocytes expressing mGluR1, mGluR3, and mGluR5. In terms of studies on endogenous mGluRs in native neurons, Tabata *et al.* (10) showed that $[Ca^{2+}]_o$ fails to induce $[Ca^{2+}]_i$ mobilization in the Purkinje cells from mGluR1 knock-out mice, whereas $[Ca^{2+}]_i$ is elevated by $[Ca^{2+}]_o$ in Purkinje cells from mGluR1α rescued mice. Furthermore, brain slice experiments from Hardingham *et al.* (11) demonstrated that $[Ca^{2+}]_o$ mediates postsynaptic efficacy via activation of group I mGluRs. Taken together, these studies represent strong evidence that $[Ca^{2+}]_o$ is a physiologically relevant modulator of mGluR1α activity in the central nervous system. Based on mutational analyses, the Ca^{2+}- and Glu-binding sites were postulated to be close to one another but not completely overlapping (6). For example, S166D decreases $[Ca^{2+}]_i$ re-

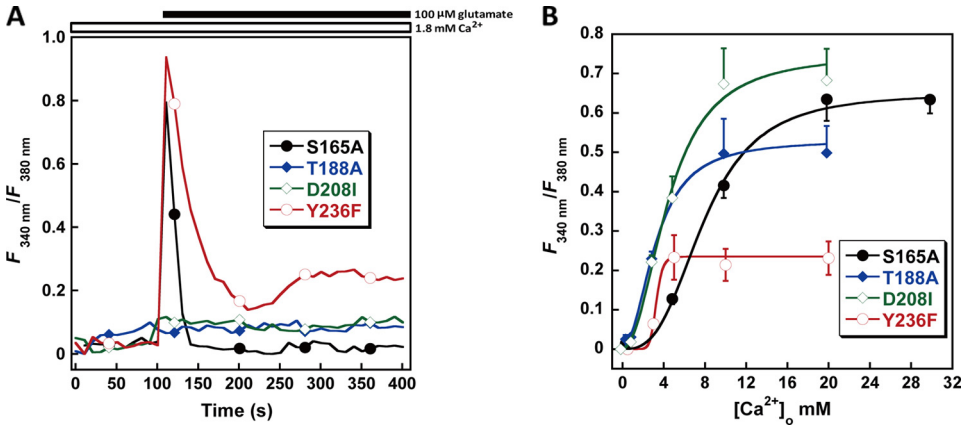

FIGURE 8. **Receptors with mutations in the Glu-binding pocket can sense Ca^{2+} but not Glu in physiological buffer.** Four residues from the reported Glu-binding pocket were selected to mutate into non-polar residues. Intracellular Ca^{2+} levels indicated by Fura-2 were recorded using fluorescence microscopy, which detected the ratio of the emission at 510 nm with excitation at 340 and 380 nm. *A*, T188A and D208I abolish sensitivity to Glu, but S165A and Y236F still respond to 100 μM Glu. *B*, mutants S165A, T188A, D208I, and Y236F remain capable of responding to $[Ca^{2+}]_o$; the maximal responses of S165A, T188A, and D208I are comparable with that of WT mGluR1α, whereas Y236F decreases the sensitivity of the receptor to $[Ca^{2+}]_o$ ($n = 3$).

TABLE 3
$[Ca^{2+}]_i$ response of mutants in Glu-binding site ($n = 3$)

Mutants	EC_{50}	n_{Hill}	Maximal response[a]
	mM		%
S165A	8.1	3.1	86 ± 3
T188A	3.4	2.2	74 ± 2
D208I	4.6	2.3	95 ± 3
Y236F	3.3	10.9	33 ± 3

[a] Maximal responses are normalized to the maximal response of wild type mGluR1α to Glu.

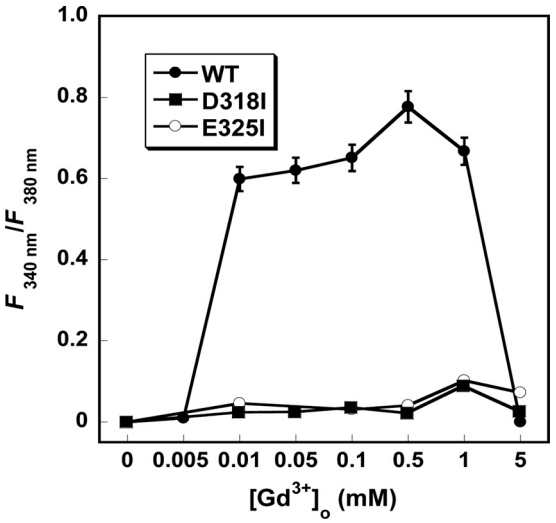

FIGURE 9. **Mutations D318I and E325I in the predicted Ca^{2+}-binding site abolish $[Ca^{2+}]_i$ responses of the receptor to $[Gd^{3+}]_o$.** HEK293 cells expressing D318I, E325I, and WT mGluR1α were preincubated in 140 mM NaCl, 4 mM KOH, 10 mM HEPES, 1.5 mM Ca^{2+}, 1 mM $MgCl_2$, and 10 mM glucose, pH 7.5, for up to 1.5 h before fluorescence microscopy was carried out. Gd^{3+} was added into the loading buffer (140 mM NaCl, 4 mM KOH, 10 mM HEPES, and 0.3 $MgCl_2$, pH 7.4) in the perfusion system. $[Ca^{2+}]_i$ levels indicated by Fura-2 are presented by the ratio of the fluorescence at 510 nm when excited at 340 and 380 nm as above. The $[Ca^{2+}]_i$ response of wild type mGluR1α displays a bell-shape curve, but D318I and E325I completely abolish $[Ca^{2+}]_i$ release to $[Gd^{3+}]_o$ ($n = 3$).

sponses (6) and lowers sensitivity to Glu (39). Our data show that S166A maintains sensitivity to $[Ca^{2+}]_o$ albeit with reduced responsiveness (Fig. 4*C*). This residue is located at the ECD hinge joint but away from our predicted site in the flexible hinge region (Fig. 1*B*). The observed decrease in mGluR1α sensitivity observed with S166D could be a result of tuning the Ca^{2+} binding affinity and Ca^{2+}-induced conformational change by altering electrostatic interactions around the predicted Ca^{2+}-binding site (40).

As shown in Fig. 1*C*, the predicted Ca^{2+}-binding residue Asp-322 is conserved in group I mGluRs. Glu-325 is highly conserved in group I (mGluR1 and mGluR5) and group II (mGluR2 and mGluR3) mGluRs (Fig. 1*C*). Interestingly, mGluR5 in group I and mGluR3 in group II sense $[Ca^{2+}]_o$ at physiological levels, whereas mGluR2 is activated only when $[Ca^{2+}]_o$ is more than 10 mM (6). On the basis of our observation that E325I abolished Ca^{2+}-induced responses for mGluR1α but retained responsiveness to Glu, we concluded that Glu-325 might be very important for Ca^{2+} binding in the mGluR family generally. Analysis by the Contacts of Structural Units server indicates that Glu-325 interacts electrostatically with Arg-297 and Arg-323 in the Glu-bound structures of mGluR1α (41), suggesting that Glu-325 stabilizes the local structure through an electrostatic interaction. As revealed by the grafting approach (Fig. 2*A*), E325I significantly reduces the Ca^{2+}-binding ability in mGluR1α, possibly by disturbing the favorable local charge environment.

Fig. 1*C* shows that Asp-318 in mGluR1α, located at the hinge region, is conserved in all members of the three GPCRs, corresponding to Asp-295 of mGluR2, Asp-301 of mGluR3, Asp-309 of mGluR8, and Glu-297 of CaSR (23, 24, 42). Figs. 4 and 6 clearly demonstrate that Asp-318 contributes not only to Ca^{2+}- but also Glu-triggered $[Ca^{2+}]_i$ responses. This residue seems to play an essential role in the activation of mGluRs. Consistent with this finding, a D318A mutation was shown previously to reduce receptor expression on the membrane and abolish Glu-triggered $[Ca^{2+}]_i$ and inositol trisphosphate responses (25).

Our findings also appear to be applicable to other members of the three GPCRs, especially CaSR. The mutation E297I in CaSR, equivalent to D318I in mGluR1α, impairs receptor activation (23, 24, 42). Glu-297 is an important residue in our reported Ca^{2+}-binding site in the CaSR hinge region (23, 24); the mutant E297I significantly impairs sensitivity to $[Ca^{2+}]_o$ with an EC_{50} of 9.6 ± 0.2 mM $[Ca^{2+}]_o$. Mutations at or around this Ca^{2+}-binding site are also associated with clinical syndromes (autosomal dominant hypocalcemia and familial hypocalciuric hypercalcemia) because of either an increase or a decrease in the sensitivity of the respective receptors to $[Ca^{2+}]_o$. Zhang *et al.* (43) and others (44, 45) have also reported that mutations around this site, Ser-147, Ser-170, Asp-190, Tyr-218, and E297K, impair the activation of human CaSR by $[Ca^{2+}]_o$. Recently Silve *et al.* (42) have shown that the missense mutations E297K and Y218S significantly reduce the maximal response of the CaSR. Although E297K was considered a key factor in impairing protein folding, thus leading to lower expression on the cell surface and impaired responsiveness to $[Ca^{2+}]_o$, our unpublished data[3] show that E297I has a membrane expression level comparable with that of the wild type CaSR. Therefore, the low expression level of E297K could be, at least in part, the result of the substitution of an unfavorable positive charge, which modifies the local charge balance, leading to reduced folding efficiency. Furthermore, our assessment of the surface expression of D318I by flow cytometry showed that it was at the same level as wild type; this echoes the impact of mutating the equivalent residue in CaSR (*e.g.* Glu-297). It has been postulated that residues Ser-170, Asp-190, Gln-193, Ser-296, and Glu-297 are critical for Ca^{2+} binding to CaSR and functionality of the receptor (42), which is in excellent agreement with our prediction. In addition, CaSR functions primarily as a $[Ca^{2+}]_o$-sensing receptor but can also integrate information about protein metabolism (*i.e.* amino acids) with that of divalent cations (*e.g.* calcium) (46). CaSR displays sensitivity to amino acids, especially phenylalanine and other aromatic amino acids, likely via three serine residues (Ser-169—Ser-171) at a site corresponding to the Glu-binding pocket in mGluR1α. The double mutation T145A/S170T specifically abolishes CaSR responsiveness to amino acids while leaving $[Ca^{2+}]_o$ sensing intact (47). Our unpublished data[5] show that Ca^{2+} and phe-

[3] C. Zhang and J. Yang, unpublished work.

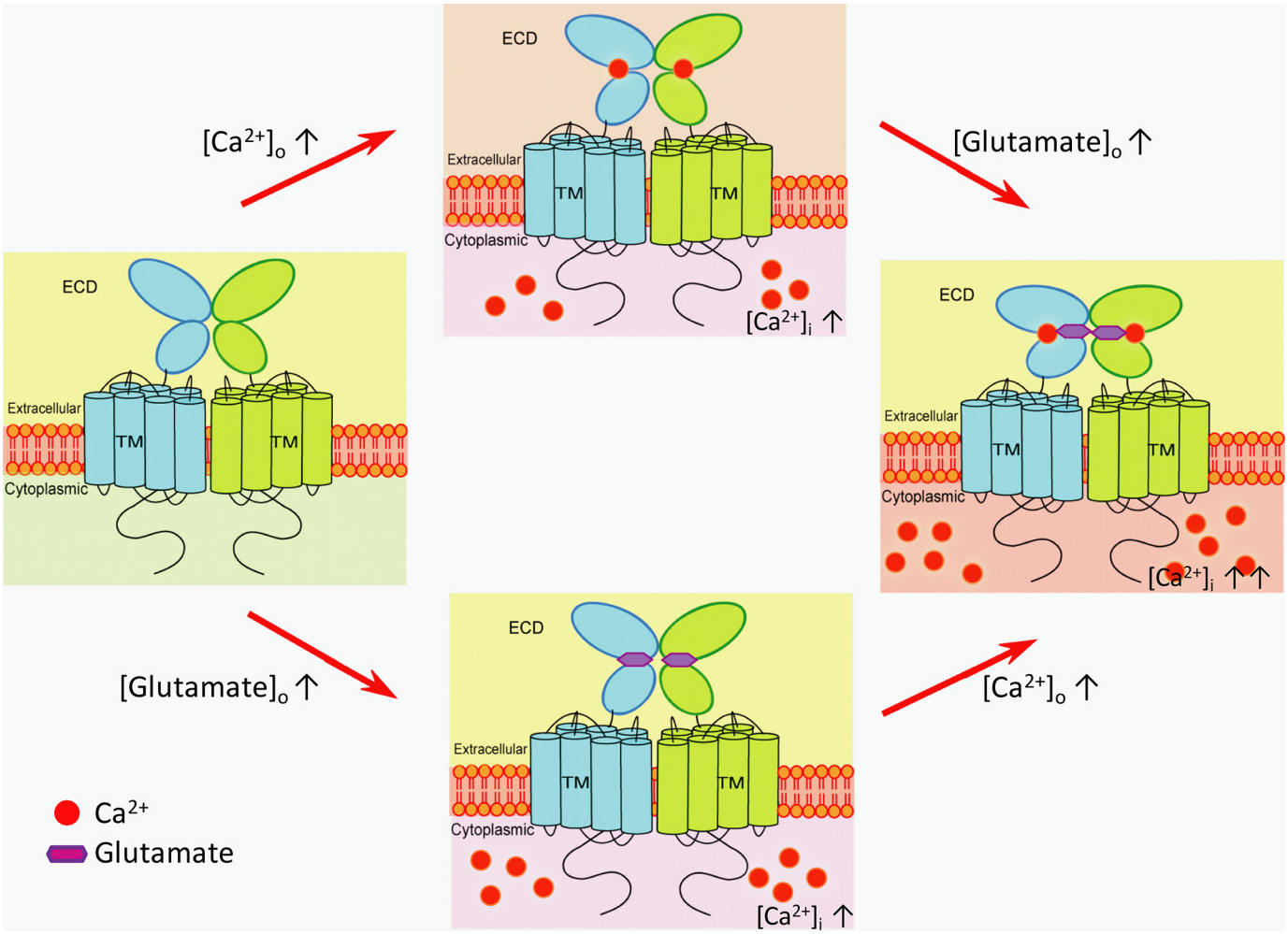

FIGURE 10. **A dual activation model for mGluR1α involving both extracellular Ca^{2+} and Glu via the overlapping and interacting binding pockets for the two ligands at the hinge region of the ECD.** Increasing either Glu or $[Ca^{2+}]_o$ partially activates mGluR1α. However, full activation of intracellular Ca^{2+} signaling by mGluR1α requires the simultaneous binding of both Glu and Ca^{2+}; Asp-318 plays a key role in the synergy between the two agonists. In this sense, mGluR1α can be viewed as a coincidence detector, requiring the binding of both ligands for maximal intracellular signaling.

nylalanine also synergistically modulate the signaling functions of CaSR.

In summary, we have predicted and confirmed experimentally a calcium-binding site in the extracellular domain of mGluR1α. We have also shed new light on the co-activation of mGluR1α by Glu and $[Ca^{2+}]_o$. These findings provide novel perspectives on mGluR1α, which may be viewed as capable of integrating information from two very different types of ligands (an amino acid neurotransmitter and a divalent cation). The levels of $[Ca^{2+}]_o$ in the brain are highly dynamic (37), and the affinity constants that we have determined in our studies on calcium binding to mGluR1α are well within the dynamic, physiological range of $[Ca^{2+}]_o$ in the brain. For family 3 GPCRs other than CaSR, the physiological importance of $[Ca^{2+}]_o$ binding has been uncertain; but the findings reported here may be useful in resolving this mystery by allowing for the development of knock-in mutations to mGluR1α, and resultant mouse models, that disrupt the ability of the receptor to bind $[Ca^{2+}]_o$ while leaving Glu binding intact. Moreover, because many of the key calcium-binding residues defined in our studies are conserved for other family 3 GPCRs, our findings may have relevance for a host of other receptors beyond just mGluR1α (6, 7). Family 3 GPCRs have tremendous potential as therapeutic targets, and therefore the advances described here may facilitate the development of novel family 3 GPCR-targeted drugs for use in the treatment of many different diseases.

Acknowledgments—We thank Chen Zhang for supporting our work with her unpublished data, Dr. Deep Shukla for calculating the combination indices, Dr. Kasper Hansen for suggestions on experimental design, and Drs. Keqiang Ye and Paul F. Worley for providing mGluRs plasmids.

REFERENCES

1. Kano, M., and Kato, M. (1987) *Nature* **325,** 276–279
2. Kaupmann, K., Huggel, K., Heid, J., Flor, P. J., Bischoff, S., Mickel, S. J., McMaster, G., Angst, C., Bittiger, H., Froestl, W., and Bettler, B. (1997) *Nature* **386,** 239–246
3. Nakanishi, S. (1994) *Neuron* **13,** 1031–1037
4. Masu, M., Tanabe, Y., Tsuchida, K., Shigemoto, R., and Nakanishi, S. (1991) *Nature* **349,** 760–765
5. Conn, P. J., and Pin, J. P. (1997) *Annu. Rev. Pharmacol. Toxicol.* **37,** 205–237
6. Kubo, Y., Miyashita, T., and Murata, Y. (1998) *Science* **279,** 1722–1725
7. Kniazeff, J., Bessis, A. S., Maurel, D., Ansanay, H., Prézeau, L., and Pin, J. P.

(2004) *Nat. Struct. Mol. Biol.* **11,** 706–713
8. Kubokawa, K., Miyashita, T., Nagasawa, H., and Kubo, Y. (1996) *FEBS Lett.* **392,** 71–76
9. Tabata, T., and Kano, M. (2004) *Mol. Neurobiol.* **29,** 261–270
10. Tabata, T., Aiba, A., and Kano, M. (2002) *Mol. Cell. Neurosci.* **20,** 56–68
11. Hardingham, N. R., Bannister, N. J., Read, J. C., Fox, K. D., Hardingham, G. E., and Jack, J. J. (2006) *J. Neurosci.* **26,** 6337–6345
12. Kawabata, S., Kohara, A., Tsutsumi, R., Itahana, H., Hayashibe, S., Yamaguchi, T., and Okada, M. (1998) *J. Biol. Chem.* **273,** 17381–17385
13. Nash, M. S., Saunders, R., Young, K. W., Challiss, R. A., and Nahorski, S. R. (2001) *J. Biol. Chem.* **276,** 19286–19293
14. Tsuchiya, D., Kunishima, N., Kamiya, N., Jingami, H., and Morikawa, K. (2002) *Proc. Natl. Acad. Sci. U. S. A.* **99,** 2660–2665
15. Kunishima, N., Shimada, Y., Tsuji, Y., Sato, T., Yamamoto, M., Kumasaka, T., Nakanishi, S., Jingami, H., and Morikawa, K. (2000) *Nature* **407,** 971–977
16. Muto, T., Tsuchiya, D., Morikawa, K., and Jingami, H. (2007) *Proc. Natl. Acad. Sci. U. S. A.* **104,** 3759–3764
17. Abe, H., Tateyama, M., and Kubo, Y. (2003) *FEBS Lett.* **545,** 233–238
18. Tateyama, M., Abe, H., Nakata, H., Saito, O., and Kubo, Y. (2004) *Nat. Struct. Mol. Biol.* **11,** 637–642
19. Kirberger, M., Wang, X., Deng, H., Yang, W., Chen, G., and Yang, J. J. (2008) *J. Biol. Inorg. Chem.* **13,** 1169–1181
20. Yang, W., Wilkins, A. L., Ye, Y., Liu, Z. R., Li, S. Y., Urbauer, J. L., Hellinga, H. W., Kearney, A., van der Merwe, P. A., and Yang, J. J. (2005) *J. Am. Chem. Soc.* **127,** 2085–2093
21. Deng, H., Chen, G., Yang, W., and Yang, J. J. (2006) *Proteins* **64,** 34–42
22. Wang, X., Kirberger, M., Qiu, F., Chen, G., and Yang, J. J. (2009) *Proteins* **75,** 787–798
23. Huang, Y., Zhou, Y., Castiblanco, A., Yang, W., Brown, E. M., and Yang, J. J. (2009) *Biochemistry* **48,** 388–398
24. Huang, Y., Zhou, Y., Yang, W., Butters, R., Lee, H. W., Li, S., Castiblanco, A., Brown, E. M., and Yang, J. J. (2007) *J. Biol. Chem.* **282,** 19000–19010
25. Sato, T., Shimada, Y., Nagasawa, N., Nakanishi, S., and Jingami, H. (2003) *J. Biol. Chem.* **278,** 4314–4321
26. Falke, J. J., Drake, S. K., Hazard, A. L., and Peersen, O. B. (1994) *Q. Rev. Biophys.* **27,** 219–290
27. Glusker, J. P. (1991) *Adv. Protein Chem.* **42,** 1–76
28. Honig, B., and Nicholls, A. (1995) *Science* **268,** 1144–1149
29. Nicholls, A., Sharp, K. A., and Honig, B. (1991) *Proteins* **11,** 281–296
30. Sali, A., and Blundell, T. L. (1993) *J. Mol. Biol.* **234,** 779–815
31. Ye, Y., Lee, H. W., Yang, W., Shealy, S. J., Wilkins, A. L., Liu, Z. R., Torshin, I., Harrison, R., Wohlhueter, R., and Yang, J. J. (2001) *Protein Eng.* **14,** 1001–1013
32. Ye, Y., Lee, H. W., Yang, W., Shealy, S., and Yang, J. J. (2005) *J. Am. Chem. Soc.* **127,** 3743–3750
33. Ye, Y., Shealy, S., Lee, H. W., Torshin, I., Harrison, R., and Yang, J. J. (2003) *Protein Eng.* **16,** 429–434
34. Shaw, G., Morse, S., Ararat, M., and Graham, F. L. (2002) *FASEB J.* **16,** 869–871
35. Chou, T. C., and Hayball, M. P. (1996) *CalcuSyn, Windows Software for Dose Effect Analysis*, Biosoft, Cambridge
36. Abe, H., Misaka, T., Tateyama, M., and Kubo, Y. (2003) *Mol. Cell. Neurosci.* **23,** 157–168
37. Vassilev, P. M., Mitchel, J., Vassilev, M., Kanazirska, M., and Brown, E. M. (1997) *Biophys. J.* **72,** 2103–2116
38. Francesconi, A., and Duvoisin, R. M. (2004) *J. Neurosci. Res.* **75,** 472–479
39. Miyashita, T., and Kubo, Y. (2000) *Receptors Channels* **7,** 25–40
40. Jones, L. M., Yang, W., Maniccia, A. W., Harrison, A., van der Merwe, P. A., and Yang, J. J. (2008) *Protein Sci.* **17,** 439–449
41. Sobolev, V., Sorokine, A., Prilusky, J., Abola, E. E., and Edelman, M. (1999) *Bioinformatics* **15,** 327–332
42. Silve, C., Petrel, C., Leroy, C., Bruel, H., Mallet, E., Rognan, D., and Ruat, M. (2005) *J. Biol. Chem.* **280,** 37917–37923
43. Zhang, Z., Qiu, W., Quinn, S. J., Conigrave, A. D., Brown, E. M., and Bai, M. (2002) *J. Biol. Chem.* **277,** 33727–33735
44. Tu, C. L., Oda, Y., Komuves, L., and Bikle, D. D. (2004) *Cell Calcium* **35,** 265–273
45. Chang, W., and Shoback, D. (2004) *Cell Calcium* **35,** 183–196
46. Breitwieser, G. E., Miedlich, S. U., and Zhang, M. (2004) *Cell Calcium* **35,** 209–216
47. Mun, H. C., Culverston, E. L., Franks, A. H., Collyer, C. A., Clifton-Bligh, R. J., and Conigrave, A. D. (2005) *J. Biol. Chem.* **280,** 29067–29072
48. Wong, X., Zhao, K., Kirberger, M., Wong, H., Chen, G., and Yang, J. (2010) *Protein Sci.* **19,** 1180–1190